BASELINE ALGORITHM DEFINITION FOR A FUTURE REAL-TIME AUTONOMOUS SENSOR SCHEDULING STRATEGY FOR SST

G. Pedone[(1)], J. Utzmann[(1)], and R. Förstner[(2)]

[(1)]*Airbus Defence and Space GmbH, 88090 Immenstaad, Germany, Email: {guido.pedone, jens.utzmann}@airbus.com*
[(2)]*Universität der Bundeswehr München, 85579 Neubiberg, Germany, Email: roger.foerstner@unibw.de*

ABSTRACT

This paper studies the Catalogue Maintenance (CM) problem from the point of view of observation planning for tracking Resident Space Objects (RSOs). Within Airbus Defence and Space a tool has been created to reduce the computational load for observation scheduling and to provide support for a future real-time scheduler. In fact, the proposed baseline does not try to allocate all the sensor tasks beforehand for the full observation period (e.g. one entire night). It evolves in a myopic state-space way, simulating just the imminent observing scenario and together with the previously collected information performs an optimization of the next task to execute, eventually to converge to an optimal coverage condition of the objects. The advantage of this approach is that it can be adopted for real-time decision-making strategies that, based on past and currently obtained measurements, may change the plan execution, compromising the forecasted optimality of a plan obtained completely offline. This paper analyses the results and comments the possible future developments for the proposed sensor tasking strategy. Finally, a comparison with state of the art scheduling optimization algorithms, from simple Greedy-Methods to the heuristic Genetic Algorithms is presented. The proposed work summarizes the implementation of the scheduler within the orbit propagation and determination tool SPOOK (Special Perturbations Orbit determination and Orbit analysis toolKit), which is developed at Airbus Defence and Space.

Keywords: SSA, Autonomous Scheduling, Optmization, Gaussian Mixtures, CPHD.

1. INTRODUCTION

Today, the congestion of some orbital regions around the Earth and the presence of numerous space debris are creating an high-risk environment for operative satellite missions. The main countermeasures that SSA activities are applying in order to avoid collisions between debris and active satellites rely on an accurate knowledge of the orbits of RSOs. The aim of Space Surveillance and Tracking (SST) is to build-up and maintain a catalogue which contains information about the detected objects, such as their orbits and physical properties [2]. CM aims to monitor and process the catalogue data in order to periodically schedule new observations. This SST process is shown in Fig.1. The quality of the cataloguing products depends on several aspects of the entire end-to-end (E2E) SST chain: sensor accuracy and sensitivity, the number of sensors and their location, minimal and optimal timelines for observations and measurement collection, fidelity of data processing (orbit determination, correlation methods) and fidelity of observation planning and scheduling. The aim of this work focuses on the last task in order to optimize observation strategies for one relevant use case: CM. The goal of CM is to optimize all the possible tracking (sensors-targets) combinations, in order to make best use of the sensors and obtain as much information as possible out of the measurements. Classical CM strategies make use of objective functions (called also cost or reward functions) to quantify the result of an observation and select the best sensor-target combination to perform tracking at each time step. Since in CM the common trade-off is between velocity of computation and fidelity of the simulation results, objective functions can be either very simple, involving for example parametrized gains as in greedy methods presented in [6] in Chapter 12, and coverage maximization [11], or more defined covariance-based gains as in [8, 9]. Furthermore, classical optimization strategies rely on the assumption of convex-shape problem formulation [11], that is not always the case or of difficult representation depending on the sample-size of objects. The nature of these methods is usually of an offline simulation of all the possible observation combinations (or a portion of it) and the evaluation of objective functions to determine the best solution. However, some recent definitions of multi-targets multi-observers filtering methods, in particular the Probability Hypotheses Density (PHD) and Cardinalized-PHD (CPHD), presented by Ronald Mahler first in 2000 [12], start being very appealing for CM. Their ability is to represent effectively the object tracking problem, that is to maintain the track-continuity of a large population of RSOs, incorporating all the sources of uncertainties for each object (or cloud of objects) in a joint coherent probabilistic representation.

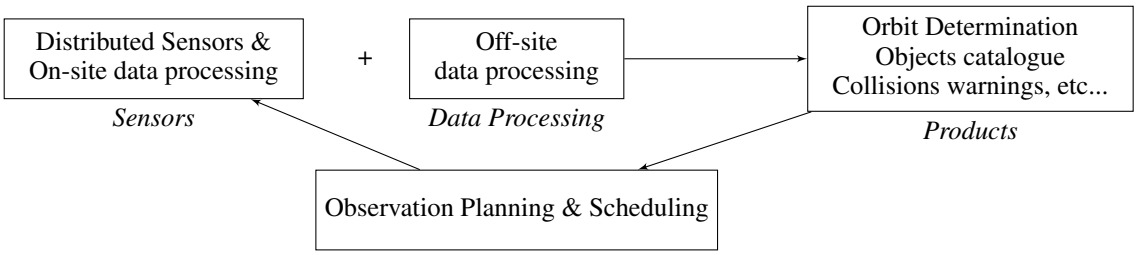

Figure 1. End-to-end chain of SST system.

This paper is proposing a possible real-time application of a CPHD-like filtering model, where a single joint dynamically evolving stochastic system, is step-by-step propagated and optimized in an observation-simulation scenario. The main idea of the proposed automatic scheduler is to operate with a myopic view of the objects propagation scenario. That means, each task is scheduled accordingly to the information of the past time steps. The overall optimization of the scheduling problem is not evaluated considering the full allocatable time, but is conducted on a step-by-step basis.
The CM strategy presented in this work, can be easily summarized in the following points:

1. first, the scheduler is fed by an initial catalogue of objects, for example retrieved from recent instances of TLE[1] objects;
2. then, with the initial catalogue of objects a mixture of Gaussian components will be defined, where each component will store the information of the mean value of the object state to which they are related and its covariance.
3. This Gaussian Mixture (GM) of objects is propagated up to the next time step accordingly to the classical rules of Gaussian Mixture Models (GMM)[20]. The length of the time step is to be considered as the length of a single sensor's task, with a granularity of intermediate propagation equivalent to the observation time frame of the sensor (e.g. the exposure time for an optical sensor).
4. For the new time step the accessibility of each GM component is then evaluated. In fig. 2 is shown as an example the visible semi-sphere of an optical ground observer. Accessibility means to evaluate if an object is crossing the visible sky over an observer (in case of a ground-based facility) or space around an observer on-orbit. The visible area of a sensor depends on physical (day-night, illuminations, etc.) and geometrical constraints (area and obstructions around an observer, dynamical models, etc.). However, the explanation of all the methods to evaluate the crossings and illuminance conditions of a target is out of the scope of this paper.

[1]Two Line Elements, it is a standard format for space object data sharing and the basis of the main RSO catalogues. In this work, TLEs will always be referred to objects retrieved from the space-track.org catalogue.

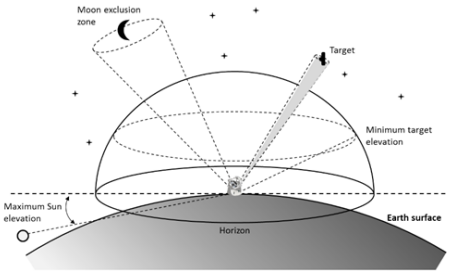

Figure 2. Accessibility sphere of a ground-based observer.

5. Once the accessibility of the GM components is evaluated, depending on the configuration of the Sensor Network (SN) a subset of all the possible combinations observer-target is selected and measurements are simulated.
6. The simulated measurements together with the information of the propagated GM will go to feed an approximated version of a CPHD filter, that will both update the uncertainty information of the GM (the covariances of each component) thanks to an UKF[2] philosophy and the intensity and cardinality of the mixture.
7. For all these combinations of observation it is evaluated a reward function to indicate the possible gain in information achievable thanks to the observation.

In the next sections, all the features and procedures described up to now are going to be fully explained. The paper is organized as follow: first a presentation of the multi-sensors and multi-targets filtering context in section 2, a presentation of the algorithm integrated inside the Airbus DS's software tool SPOOK in section 3, the analysis of some simulation results in section 4 and finally the conclusion in section 5.

2. MULTI-SENSORS MULTI-TARGETS FILTERING

Multi-targets tracking theories born to solve air-traffic (usually for radars) management problems. With the

[2]Unscented Kalman Filter.

time, see [5], [1], they have started to be considered also as possible development direction for SSA.
A general definition of the problem is given by Ronald Mahler in [14] (Chapter 12), as follow:

1. Formulate the complete set of all observers and targets as single joint dynamically evolving stochastic system using point process theory (e.g. random set theory, RDS).
2. Propagate the unknown probability density function (pdf) of the system using a recursive joint multi-sensors multi-targets Bayesian estimation.
3. Define and apply suitable reward functions that express global probabilistic goals for sensor tasking.
4. Use a valid optimization strategy to cope with the intrinsic unknowability of future observations.
5. Apply appropriate simplifications of this general (but usually intractable) formulation.

On the next sub-sections will be given a presentation of the problem for single state (or target) problem, and for analogy will be explained the definition of multi-targets and multi-sensors spaces and how the CPHD finds a suitable trade-off between the analytical solution of the problem and its tractability.

2.1. CPHD Filter

In the FISST framework for multi-targets filters one of the simplest estimator is the Probability Hypotesis Density (PHD) filter, that predicts, updates and corrects the first moment of the multi-target pdf, known also as intensity function $\nu(\cdot)$ or PHD. The CPHD filter propagates and updates also the cardinality distribution together to the first moment estimate [21]. The cardinality function is a discrete probability distribution on the number of components inside a mixture [5].
Inside this filter framework, for each component of the mixture is associated a weight ω, that corresponds to its "intensity" inside the mixture. When the uncertainties around the state are increasing, that is, the covariance is increasing, the relative weight of the component will be low, since the relative Gaussian uncertainty will be spread on more space. Vice-versa, when there is a good estimate of the state (for example after an observation), the weight of the component will be higher.

2.1.1. Problem formulation

A good introduction to the single-target filtering can be found in [20]. The first assumption that is going to be done for such formulation is to consider the space object dynamic as a partially observed Markov decision problem[3]. It is assumed, additionally, that both the predicted and updated state can be represented by independent identically distributed (IID) clusters of random finite sets (RFS).
Further assumptions for the CPHD formulation will be presented later.
The proposed description of the method will follow the one presented in [5, 20, 21]. Space objects state propagation problems can be easily considered to follow a Markov process. Inside this process, the transition from state space at time $k-1$ to the current time step k can be seen thanks to a transition function:

$$f_{k|k-1}(x_k|x_{k-1}) \ \rightarrow \ prior\ density \tag{1}$$

that represents the orbital dynamic propagation. This prior density is partially observed in the observation space through the likelihood function:

$$g_k(z_k|x_k) \ \rightarrow \ likelihood\ function \tag{2}$$

that represents the function related to measurement generation given an orbital state.
Given the measurements set, it is possible to evaluate the probability of a state after an observation:

$$p_k(x_k|z_k) \ \rightarrow \ posterior\ density \tag{3}$$

that gives us the posterior density. The posterior density p_k can be computed using the Bayes recursion:

$$\begin{aligned} p_{k|k-1}(x_k|z_{1:k-1}) &= \\ &\int f_{k|k-1}(x_k|x)p_{k-1}(x|z_{1:k-1})dx \\ p_k(x_k|z_{1:k-1}) &= \\ &\frac{g_k(z_k|x_k)p_{k|k-1}(x_k|z_{1:k-1})}{\int g_k(z_k|x)p_{k|k-1}(x|z_{1:k-1})dx} \end{aligned} \tag{4}$$

different numerical methods can be used to solve this recursion, as explained in [20].

This formulation can be easily extended to a multi-state scenario: let be $M(k)$ the number of components inside a mixture at time k and $N(k)$ the number of measurements at time k. In such framework are not considered any specific ordering rules for the states and measurements collections:

$$\begin{aligned} \boldsymbol{X}_k &= \{x_{k,1}, ..., x_{k,M(k)}\} \\ \boldsymbol{Z}_k &= \{z_{k,1}, ..., x_{z,N(k)}\}. \end{aligned} \tag{5}$$

Analogously to single-state formulation, in multi-targets formulation the state of each target or component (x_k,y_k) can be modelled as random vectors, hence, also $\boldsymbol{X}_k$ and $\boldsymbol{Z}_k$ are random finite sets (RFS). An equal recursion formulation as above can be formulated.
However, the recursion formulation in multi-targets space is computationally intractable, but adding the GMM approximation to the problem it is possible to yield a closed-form solution. This approximation assumes that targets evolve and generate measurements independently one from the other.

[3] The current state of a target depends only on the state of the last time step.

2.1.2. CPHD algorithm

The full CPHD recursion is out of the scope of this report. In this framework two simplifications have been adopted to yield the tractability of this tool: the mixture is approximated to a Gaussian Mixture Model and the number of components, as this is the case, of objects that originates the mixture (the catalogue of space objects) is considered to be known a priory. The first approximation allows to reach a closed version of the CPHD recursion [5, 7, 20, 21]. The latter simplification, on the other hand, allows to a special formulation of the filter that integrates the Unscented Kalman Filter (UKF) prediction and update procedures [21].
The Algorithm of the implemented filter is presented in [21] and [5] with respect to the intensity and cardinality recursions. However, some extensions regarding the splitting and merging (or coarsening) generations of new components have been considered during the targets propagation phase to assess the non-linearity of Gaussian assumptions needed for precise processing of orbit propagation.

3. ALGORITHM IMPLEMENTATION

This section is going to present the integration of the scheduler inside the SPOOK software tool already available in Airbus DS [4, 16]. This section will present the main building blocks of the scheduler referring to fig. 3.

3.1. Architecture of the scheduler

The baseline architecture for the automatic scheduler consists in all the loop necessary to: define a pool of objects from a catalogue, initialize a GM with the properties of the catalogues objects, propagate the objects from one time step to the next one, move the FOV, simulate/estimate measurements, perform OD on data, evaluate the reward function and choose the best pointing.
As visible from Fig. 3, the GM is defined at the beginning of the main integration loop with the a priori knowledge that we have of the objects inside the catalogue. Each integration step is made of the following phases: propagate all the objects to the next time step and evaluate the accessibility[4], select all the possible observation possibilities and evaluate for all of them the reward function associated with the observation. The observation possibility with the highest associated reward function value will be selected as next pointing for the FOV.
When a pointing position is selected, the observed objects information inside the catalogue is updated accordingly to the previously presented UKF-CPHD filter.

[4]With accessibility is meant the crossing of the object with the observable celestial sphere of the sensor, see fig. 2.

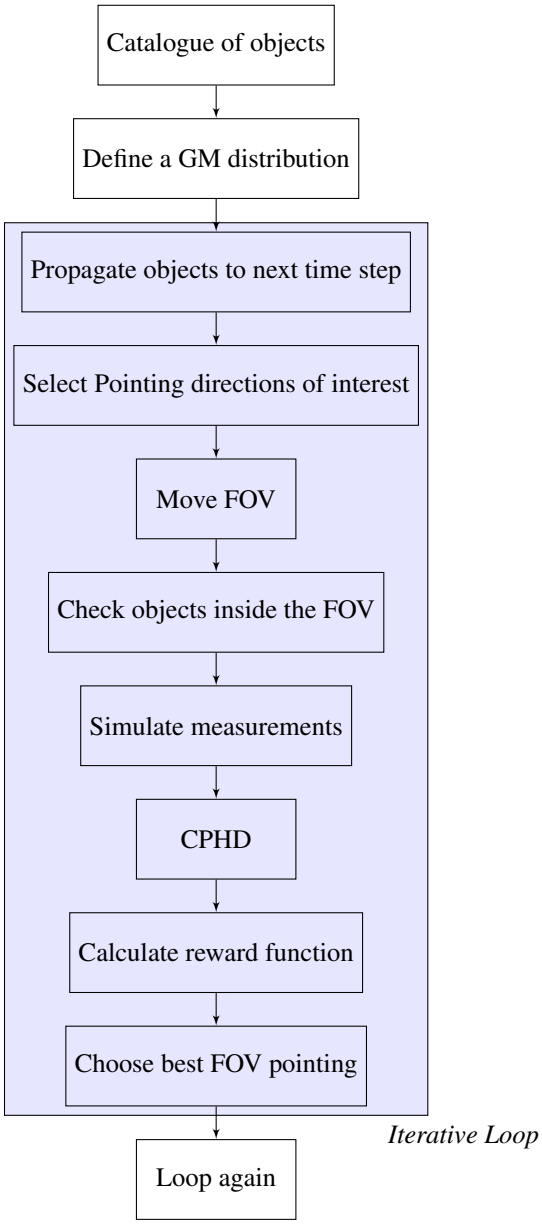

Figure 3. Baseline implementation of the automatic scheduler inside SPOOK.

3.2. Mixture propagation

The propagation of the mixture applies the UT theories, where the covariances (or uncertainties) of the objects inside the GM are updated propagating a user defined cloud of sigma points.
The propagation of the mixture relies on the already-present Airbus software called Special Perturbation Orbit Propagator (SPOP) [4]. The options for propagation can be selected by the user to different levels of accuracy. Inside the results sections, the selected options for propagation will be presented.

3.2.1. Splitting and Merging routines

Inside the GMM framework different theories for weights and components propagations can be adopted, that could be incorporated into two categories. The first idea is to not change the value of component weights during the simple propagation but only follow the splitting and merging rule when the covariance related with the states reach certain characteristics, the second idea, instead, is to have a direct influence of the uncertainty level on the weights propagation. The first method allows to save the Gaussian hypothesis, and for this reason is to be considered the most suitable when dealing with GM. In fact, the first method allows to never exceed certain value on the uncertainty or covariance by means of the so-called non-linearity index [19]. On the other side, this method can lead very easily to a huge number of components and in order to maintain a proper computational tractability a suitable components pruning routine should be applied. The second method is, instead, very suitable for big dimension problems as SST, since is not affecting in a valuable way the number of components inside a mixture.
The approach used in this work is a mixed of the previous two: for each component at each time step the non-linearity index is evaluated and used as input for the slitting and merging routines. Every time a splitting routine is triggered, the component is *virtually* split, that means, the mean value of the component state remains the same while its weight inside the mixture is reduced accordingly to the number of splitting kernels that have been evaluated. This procedure is adopted for this special case of observation scheduling, since the mean values of the object state has no sense to be modified being, in fact, a simulation and no real observations/measurements are really performed.

3.3. Measurements generation

The measurements generation routine works into two levels: estimated measurements and simulated measurements. Besides the differences in the evaluation, the first are used as reference for the CPHD filter update and are evaluated for each object for all the sigma points and the second are the results of the scheduler simulation, containing all the noise and false detection according to the simulation options.

3.3.1. Predicted Ideal Measurement Set: PIMS

In the framework of measurements simulation, a great problem is how to evaluate all the possible observation combinations given a set of catalogued objects and a network of observers. The idea at the basis of this work is to generate at each time step a Predicted Ideal Measurement Set (PIMS) taking into account the position information of the objects and their weights.
The PIMS is generated starting from the real position of the objects inside the GM and no false detections or clutters, are considered at this step, see [7] chapter 12, pag. 269.
An additional filtering has been performed on the possible combinations of observations, to obtain a feasible computational time and tractability. In fact, if considering two observers and being m and n the numbers of visible objects for the first and second sensors respectively, the total number of possible combinations is $n \cdot m$. Considering cases of ≈ 400 objects visible for each observer, the number of possible observation combinations for a big network of observers can be huge. To overcome this issue a maximum number of possible combinations per each time step has been selected, according to the lowest weights inside the mixture.

3.4. Detection prediction

The detection probability is to be evaluated as the potential position of an object to the FOV.
The probability of detection can be seen as product of two terms:

$$P_D = P_{D,sensor} \cdot P_{D,FOV} \tag{6}$$

The first term is a state-independent quantity, that represents the properties of the observer (and the images processing pipeline that is connected). This term takes into account all the instrumental errors connected with sensor performances. The exploitation of all these characteristics is out of the scope of this report. On the other hand, the second term is a state-dependent quantity, that accounts for the relative position of the mean state of the object, the FOV and its covariance.
A component of the GM is considered to be perfectly observable (ideally $P_{D,FOV} = 1$) when its estimate measurement is completely inside the FOV and the uncertainty "cloud" around that measurement is completely contained inside the FOV.
An object is considered to be partially observable when the cumulative probability density of its PDF (integrated inside the FOV) is constrained by the following values:

$$0.05 \leq \int_{FOV} p_g \left(z; z_k^j, P_{zz}^j \right) dz \leq 0.95 \tag{7}$$

A good measure of the uncertainty ($\boldsymbol{S}_k^i$) around the mean measurement can be easily given thanks to the Unscented Transformation (UT) theory:

$$\boldsymbol{S}_k^i = \sum_{l=0}^{L} u^l \left(z_{k|k-1}^l - \eta_{k|k-1}^i \right) \left(z_{k|k-1}^l - \eta_{k|k-1}^i \right)^T \tag{8}$$

where the k index indicates the time step, the indices from l to L corresponds to the components of the sigma cloud[5], u^l is the l-th component weight of the sigma cloud, η is the mean estimated measurement generated with the mean position of the object and z are the estimated measurements for all the sigma points.

[5] In this case the sigma cloud refers to the set of sigma components created accordingly to the UT theory.

The detection probability calculation has been evaluated assuming a bi-variate normal distribution of the uncertainty in the FOV space, and propagated with the Simpson's method. The bi-variate normal or Gaussian distribution is a generalization of the one-dimensional probability density function to two dimensions fields [10]. In this case the formula for the PDF evaluation is the following:

$$f(\alpha,\delta) = \frac{1}{2\pi\sigma_\alpha\sigma_\delta\sqrt{1-p^2}}\exp^{-\Theta} \qquad (9)$$
$$\Theta = \frac{1}{1-p^2}\left[\frac{(\alpha-\mu_\alpha)^2}{\sigma_\alpha^2} + \frac{(\delta-\mu_\delta)^2}{\sigma_\delta^2} - \frac{2p(\alpha-\mu_\alpha)(\delta-\mu_\delta)}{\sigma_\alpha\sigma_\delta}\right]$$

Where α and δ are the coordinates, σ_α and σ_δ the relatives uncertainties, square-roots of the diagonal elements of the matrix $\boldsymbol{S}_k^i$ of Eq. 8, and p is the correlation parameter. As the coordinates indicate, the dimension of the observables is due to the observation measurements type. In fact, considering for simplicity an optical observer, the usual reference system for measurements is expressed by means of two angles, that for consistency with standards are right ascension and declination angles.

3.5. Reward function

The proposed reward function in this work is though to be completely based on the weights information of the GM. Suitable for this case is the Renyi function, that expresses the gain in information after a possible observation (set of measurements), evaluating the improvements of the gain values after the filter update. A wide dissertation on the Renyi reward function can be found in [17].
The general formulation of the information gain is:

$$R(\boldsymbol{u}) = \frac{1}{\alpha-1}\log\int f_1(X;\boldsymbol{u})^\alpha f_0(X)^{1-\alpha}dX \qquad (10)$$

where $\boldsymbol{u}$ is the FOV control vector and $f_0(\cdot)$ and $f_1(\cdot)$ are the prior and posterior PDFs of the GM.
This formulation could be quite simplified, with the assumptions described in the previous chapter, and related completely to the weights information [17]:

$$R(\boldsymbol{u}) \approx \sum_{i=1}^{N} w_{k|k-1}^i + \frac{\alpha}{1-\alpha}\sum_{i=1}^{N} w_k^i - \frac{1}{1-\alpha}\sum_{i=1}^{N}\left(w_{k|k}^i\right)^\alpha\left(w_{k|k-1}^i\right)^{1-\alpha} \qquad (11)$$

In both Eq.s 1011, the parameter α is to be selected by the user to optimize the performances. According to the literature, and in this work, the value selected is 0.5.

4. SIMULATION SCENARIO

This section will present the results of some simulations conducted to test the performances of CM with the new real-time method and the comparison of these results with classical optimization strategies. The latter rely on the assumption that the CM problem can have a convex-shape representation. They aim to find the optimal solution (understood as possible combinations of observer-target in the time) that maximizes a certain objective function. The objective function can vary accordingly to the method used and will be presented in subsection 4.5.
The first part of this section will describe the background of the simulation: how the catalogue of object has been generated and which SN has been considered. The second part of this simulation section will describe the principal results obtained with the CPHD filter implementation for both single optical observers and a network of 2 optical sensors. Additionally, both cases of space-based observers and ground-based facilities will be considered.

4.1. Catalogue creation

For this simulations the selected objects for the catalogue creation belong to the geosynchronous class, one of the most crowded orbital region. The initial catalogue of object has been built-up using the online available TLEs for all the objects that respect the following criteria:

- for the same object there are at least 20 instances in the 30 days before the start of the simulation;
- the mean motion of the object is between 0.99 and $1.01\,\text{revolution}\,\text{d}^{-1}$;
- the eccentricity of the orbit is less than 0.001;
- and finally, the object type is one of the following two classes: Payload or debris.

The epoch of the simulation start is the 12^{th} of February 2021 at $19:00$ UTC.
As for that date, the objects that respected the previously mentioned constraints were 1076. Starting from the TLEs instances a catalogue of objects has been created, with a mean position and covariance initialization obtained with the same method described in [13] and [3].

4.2. Telescope model

During this simulation, a coarse dynamical model has been considered to take into account the steering capabilities of the sensor. Except for ART, for which a more precise dynamical model has been provided by the manufacturer and recently added into the SPOOK software, all the sensors respect a common law of $3.0\,\text{deg}/\text{s}$ in all pointing directions.

4.3. Sensors network

During these simulations four different optical sensors have been considered to highlight the performances for different selections of observer location, accuracy and FOV size. The sensor characteristics are specified in table 1. Location of the sensors have been chosen starting from existing facilities, but in order to maintain the generality of this formulation, names and characteristics have been randomly selected. Referring again to table 1, the Space-Based Optical Observer (SBOB) is a fictitious LEO object with the following mean orbital elements:

- semi-major axis, $a = 7093\,\mathrm{km}$;
- eccentricity, $e = 0.0014265$;
- inclination, $i = 98.2283°$;
- right-ascension of the ascending node, $\Omega = 150.8478°$;
- argument of the pericenter, $\omega = 129.1774°$.

The Australian Telescopes 1 and 2 (AT1 and AT2, respectively), have been chosen to test different accuracy and FOV size conditions.

4.3.1. Accessibility Analysis

For each sensor the following constraints have been applied to check the accessibility of the targets inside the initial complete catalogue presented in subsection 4.1. As visible in fig. 2, with accessibility of an object is meant the observability of the target by a certain observer during all the simulation time. The constraints applied in this framework are:

- that the object must be illuminated by the Sun or being in the penumbra;
- for ground sensors: the Sun shall be below the nautical night elevation of $-9°$;
- for ground sensors: the target shall be between $20°$ and $85°$ of elevation;
- finally, for space sensors: the target shall not be obstructed by the Earth with a limb of $150\,\mathrm{km}$ over the surface.

Fig.s 4 and 6, highlight the visibility constraints for the ground-based observers in a specific instant of time.

4.4. CPHD results

This subsection presents the main results of the simulations conducted within this project. The start of the simulation is the same specified in subsection 4.1, and the duration of the simulation is 7 days.
The objects propagation is the most time consuming step of the all the simulation. In particular, considering that starting from an initial catalogue of 1076 objects, during the propagation phase $2n_{states} + 1 = 13$[6] times the objects are propagated according to the UT theory.
For the propagation has been used 2-body model for gravity perturbations and solar radiation pressure for disturbances.
Before the overall observation-scheduling simulation, a simple accessibility analysis has been conducted for all the observers and all the targets inside the initial catalogue of 1076 objects, to see how many objects are really observable by the specific sensor or SN. The results of this investigation are present in tab. 2, together with the detection results obtained with the CPHD scheduler. In this case, with *detected objects* is meant that the object has been maintained inside the catalogue. The first two simulations have been done with a single observer configuration, to test the different coverage conditions for two sensor configurations: in-space and on-ground. The fig.s 4 and 5, represent the coverage conditions for the sensor ART and SBOB respectively. Table 2, shows that the ratio of coverage[7] for the ART case is 100.0%. However, not all of these objects are directly tracked or scheduled to be tracked, by the scheduler. In fact, due to the high density of objects, especially in the $0°$ declination area, some objects will fall inside the FOV of the sensor even when not tracked, that is, the telescope is not pointing directly to them but to an object next to them.
Fig. 6 shows, on the other hand, the coverage results of the network of sensors composed by ART, AT1 and AT2 sensors. In fig. 7 is presented the covariance trend of the ART sensor scheduling simulation for 7 days. Similar results can be shown for other two simulations with AT1, AT2 and SBOB. In particular in fig. 8, it is visible the trend of the mean position and velocity errors for all the observation configurations in tab. 2. The mean trend depends on several factors, as the scheduler configuration or the sensor properties. SN configurations, e.g. ART and the Australian observers, can have huge number of observation combinations as specified in subsection 3.3.1. The selection of pointing directions at each time step is so reduced for every observer inside the network. This setting explains the peaks $\approxeq 60\,\mathrm{km}$ of the SN configuration at the beginning of the simulation. A better sensor resolution, instead, leads to a smaller covariance envelope at the end of the simulation.

[6] with n_{states} the number of states inside the state vector

[7] The coverage ratio is the number of observed objects over the total number of visible objects during all the propagation $coverage = N_{observed}/N_{visible}$.

Table 1. Characteristics of the sensors used during the simulations:

Name	Coordinates	FOV dimension	Sensor accuracy
ART	$-6.63°$W $38.22°$N	$\varnothing = 2\,\text{deg}, 2\,\text{deg}$	$\sigma_\alpha = 1'',\sigma_\delta = 1''$
AT1	$150.0°$W $-31.0°$N	$\varnothing = 3.4\,\text{deg}, 3.4\,\text{deg}$	$\sigma_\alpha = 2'',\sigma_\delta = 2''$
AT2	$133.87°$W $-23.70°$N	$\varnothing = 2\,\text{deg}, 2\,\text{deg}$	$\sigma_\alpha = 0.5'',\sigma_\delta = 0.5''$
SBOB	Sun-synchronous orbit at $715\,\text{km}$ altitude	$\varnothing = 3.0\,\text{deg}, 3.0\,\text{deg}$	$\sigma_\alpha = 0.5'',\sigma_\delta = 0.5''$

Table 2. Coverage performances of the CPHD scheduler for different sensors and SN configurations:

observer or SN	total objects	visible objects	detected objects
ART	1076	342	342 (100.0%)
SBOB	1076	1076	1075 (99.9%)
SN: ART + AT1	1076	674	674 (100.0%)
SN: ART + AT1 + AT2	1076	761	759 (99.7%)

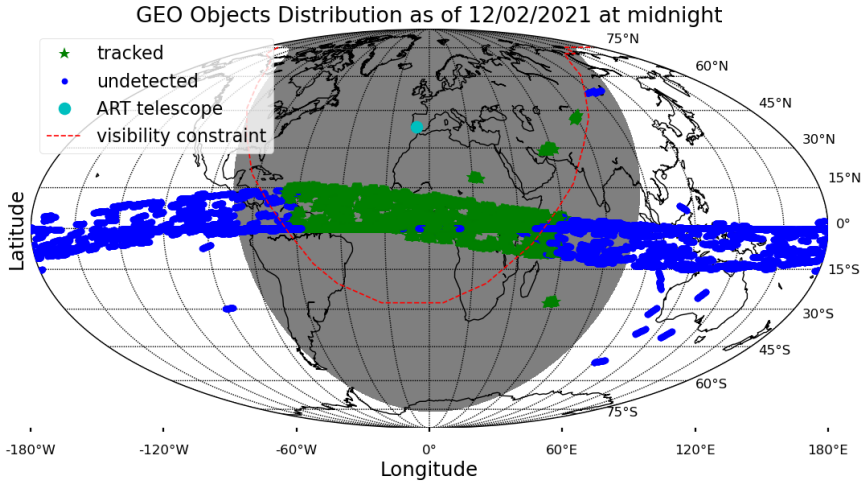

Figure 4. This figure shows the positions of all the objects inside the catalogue used for the simulation of the cphd filter. These positions refer to a small propagation of their orbits for few hours starting from the 12^{th} of February at midnight. The cyan spot represents the position of the ART telescope in Extremadura, Spain. The red dashed line indicates the limit of accessibility of the ART observer, in particular, for the $20°$ elevation constraint. The objects represented in blue describe the full GEO catalogue used for the simulation, while the green objects correspond to the actually detected targets during the 7 days of simulation.

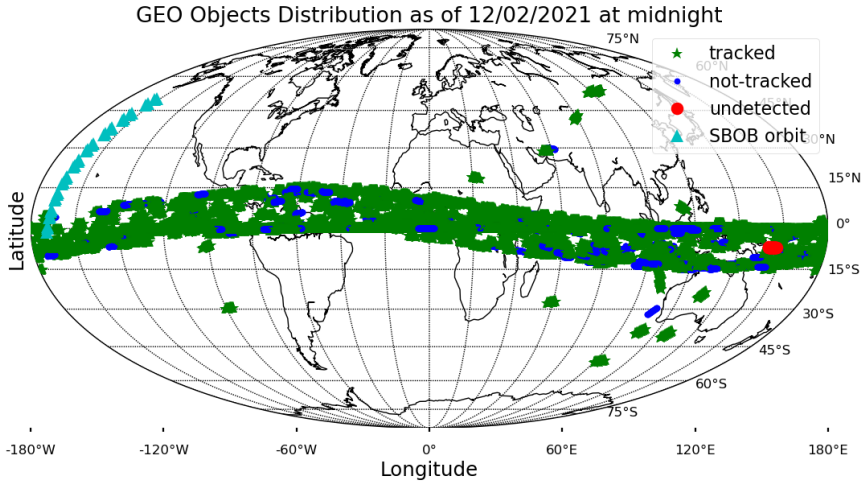

Figure 5. This figure shows the positions of all the objects inside the catalogue used for the simulation of the cphd filter. These positions refer to a small propagation of their orbits for few hours starting from the 12^{th} of February at midnight. The cyan triangle spots represent the position of the SBOB telescope in-orbit. The objects represented in blue describe the full GEO catalogue used for the simulation, while the green objects correspond to the actually detected targets during the 7 days of simulation. The red objects are the objects that the algorithm did not manage to maintain inside the catalogue.

4.5. Comparison with other methods

This subsection will present some results of observation scheduling done with other methods: a greedy method and genetic algorithm. Both methods are offline scheduling strategies that try to optimize specific cost functions. The two strategies are initialized by a list of observation requests covering the whole scheduling time (e.g. the observation night). Each request corresponds to a specific object to observe, and it is defined by a start and finish time. In the SPOOK implementation, each request is also represented by a specific observation benefit which can represent a priority gain related with the observation (e.g. scientific interest, military assets, etc..). However, for these simulations the initial benefit initialization has been set to 1 equally for every observation request. A detailed presentation of the "telescope scheduling problem", and both methods implemented in SPOOK is given in [15].

4.5.1. Greedy method

In the framework of dynamic programming, a greedy method is a method that aims to reduce considerably the computational time of the scheduling problem. The algorithm itself involves the partition of a big problem into smaller sub problems, reducing the computational time of a n-dimension problem into an $On(n)$ of time.

The algorithm is composed into two steps: sorting the requests and the main optimization loop. To start, the list of requests is initially sorted, involving recursive functions like in-place quick-partition algorithms [6, 15], accordingly to increasing final time of the request. Then, inside the main loop, for each sorted requested is evaluated the observation predecessor. The predecessor of an observation corresponds to the first observation request that is possible to perform before that observation.
For each sorted request is so evaluated the benefit of the observation, accordingly to the following rules:

- Maximum coverage: observe as many objects as possible.
- Follow-up service: maintain track of the objects with re-observations.
- Close passages: observe more objects inside the same FOV.
- Proximity with the previous observation: minimize the slewing time or the angular distance, with the previous observation.

Finally, the optimal observation is evaluated thanks to the greedy rule:

$$B(i) = max\left(B(i-1), b_i + B(P(i))\right) \qquad (12)$$

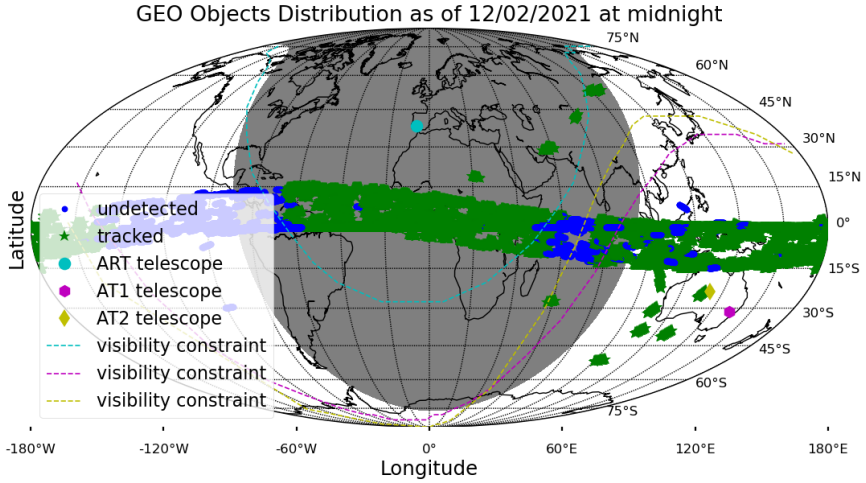

Figure 6. This figure shows the positions of all the objects inside the catalogue used for the simulation of the cphd filter. These positions refer to a small propagation of their orbits for few hours starting from the 12^{th} of February at midnight. The cyan spot represents the position of the ART telescope in Extremadura, Spain. The yellow spot corresponds to the AT2 sensor in Australia. The purple spot, instead, corresponds to the AT1 observer. The dashed lines indicate the limit of accessibility for the three observers, in particular, for the $20°$ elevation constraint. Each line has the same colour as the sensor to which it refers. The objects represented in blue describe the full GEO catalogue used for the simulation, while the green objects correspond to the actually detected targets during the 7 days of simulation.

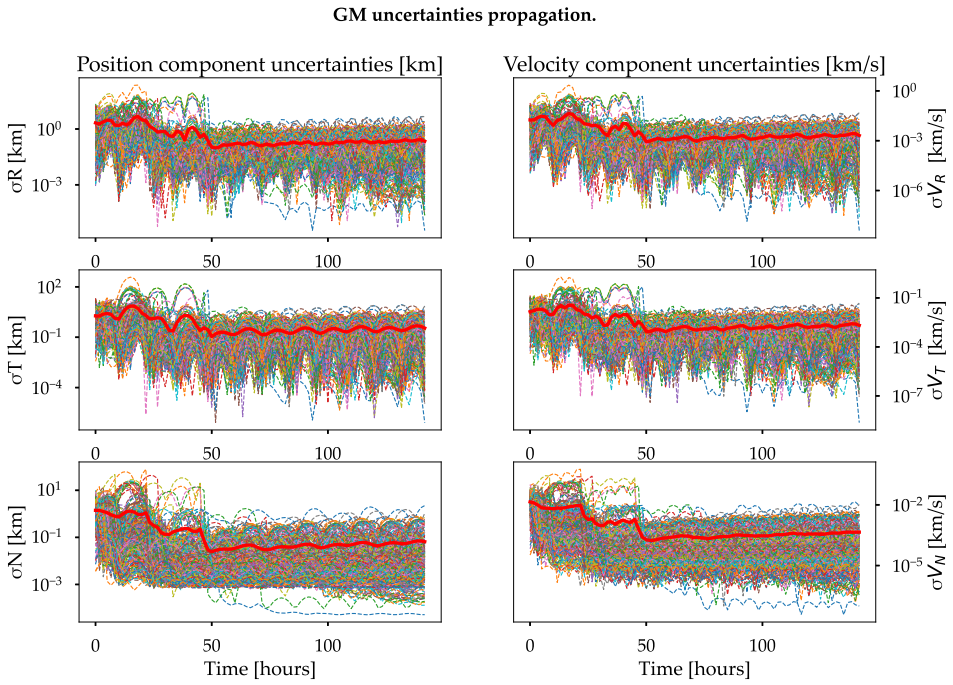

Figure 7. This figure shows the uncertainty trends of all the GM of objects during the 7 nights of propagation. Each plot corresponds to a direction in position and velocity of the RTN frame: the radial, the tangential and the normal directions. The smaller and dashed lines are for all the objects propagated by the filter, while the ticker red line is the mean value line at each time step for all the objects.

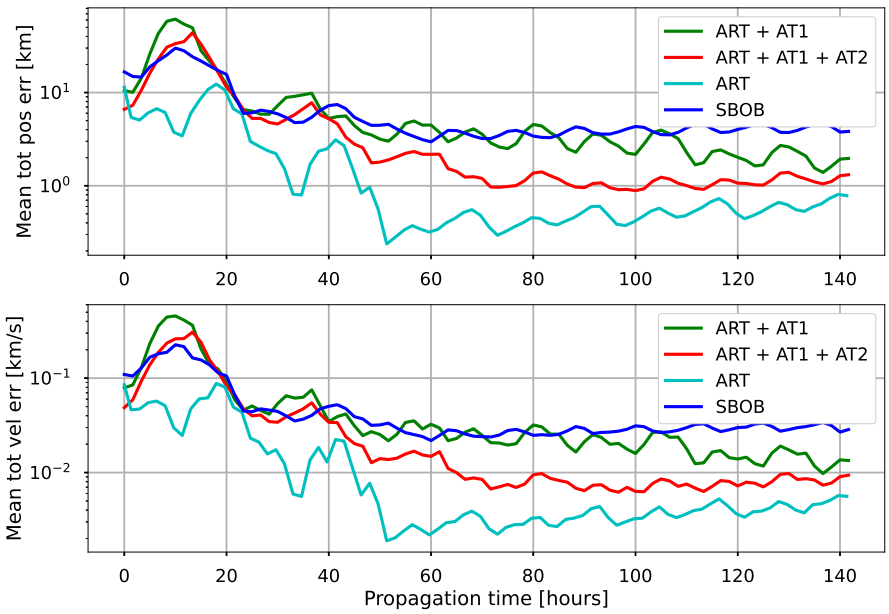

Figure 8. The mean covariance trends for the four observation configurations presented in tab. 2. The mean trend corresponds to the average value of all the norm of the diagonal elements of all the covariances of the accessible objects relative to the observer configuration.

Where $B(i)$ is the total benefit associated with the i-th scheduled observation, b_i is the benefit of the current observation requested analysed inside the loop and $P(i)$ is the index of the request predecessor. The intuitive greedy rule can be explained with the following question: *is it better to perform the previous observation request, or the current one and its predecessor?* After this main loop is completed, the observation schedule is automatically generated.

4.5.2. Genetic algorithm

The genetic algorithm (ga) belongs to the heuristic optimization methods class. In the current SPOOK implementation it makes use of a dedicated binary encoding logic where each individual, inside a population of possible scheduling solutions, corresponds to a possible observation plan made of pointing requests for each specific time step. A detailed description of the implementation of this method is provided by the author in [15]. Referring to the classical genetics terms, the size of a population corresponds to the number of observing tasks (the number of time steps during an observation night) and the number of genes is the total number of accessible objects.
The method evaluates the overall benefit of an observation plan (fitness of a population) with the following objective function:

$$fitnessvalue = \sum_{i=1}^{n_w} SIC_i \tag{13}$$

whit SIC:

$$SIC_i = \frac{1}{2} \ln \left(\boldsymbol{P}_{i-} \boldsymbol{P}_{i+}^{-1} \right) \tag{14}$$

Where SIC, is the Shannon Information Content [9, 15], the i index correspond to the i-th observation window, n_w is the number of observation windows and $\boldsymbol{P}$ is the object covariance matrix $-$ prior and $+$ after the measurement UKF update.

4.5.3. Comparison results

Simulations have been conducted for single-observer configurations for both cases. Figure 9 shows the results of two single-observer simulations performed with ART and SBOB observers. As visible, the CPHD method grants in both cases better performances in averaged accuracy of the object mixture. The greedy-method instead, is very conditioned by the high number of not-observed objects, which covariance trend tends to be dominant. Additionally, due to a fast saturation of the available memory, the simulations have been performed for three days for the ART observer and one single day for SBOB. Tables 3 and 4, show the coverage performances of the three methods. However, the coverage is not the only parameter that should be taken into account in CM, since also the correct timing to perform a certain observation should be considered. The dimension of the scheduling problem can be defined as number of observation windows $N_{windows}$ times the number of objects $N_{objects}$. Considering that the simulations have been set to perform each observation every 3 minutes, the scheduling dimension of three days simulations for ART and one day for SBOB is around half million. Computationally speaking, the greedy method is the best method for observation scheduling. The dimension of the problem, which can be defined as number of observation windows times the number of objects, is not completely exploited with the greedy method where only the number of actually observable requests is taken into account. Despite the intuitiveness of this method, the main drawback is the extreme simplification of the cost function which does not take into account information gain of an observation. The genetic algorithm, on its side, can be very efficient for small-sized problems (e.g. one night telescope scheduling), but it requires high memory resources when the number of objects to maintain is high. In fact, as said, it makes use of a dedicated binary encoding where the number of bits n_{bits}(also referred as alleles in genetics) is directly related by the number of objects $n_{objects}$ and is given by: $n_{bits} = floor\left(\log(n_{objects})\right) + 1$.

Table 3. Coverage performances for the three scheduling methods presented in subsection 4.5, for the ground-observer ART:

		3 nights simulation		
observer	$N_{objects}$	CPHD	ga	greedy
ART	342	98.2%	97.1%	80.4%

Table 4. Coverage performances for the three scheduling methods presented in subsection 4.5, for the space-observer SBOB:

		1 night simulation		
observer	$N_{objects}$	CPHD	ga	greedy
SBOB	1076	65.5%	82.4%	27.5%

5. CONCLUSIONS

This paper has presented the baseline implementation of a real-time scheduler for CM inside the Airbus DS's software tool SPOOK. The baseline implementation makes use of a CPHD filter that easily manages to keep track of the pdfs of a Gaussian mixtures of objects. Several assumptions have been considered for its implementation, and their applicability to the CM context for SSA has been explained within this paper. The filter manages to task efficiently a network of sensors in order to maintain with a certain uncertainty envelope a catalogue of objects. Despite the basic implementation that has been presented, the power of this baseline strategy is to allow a series of

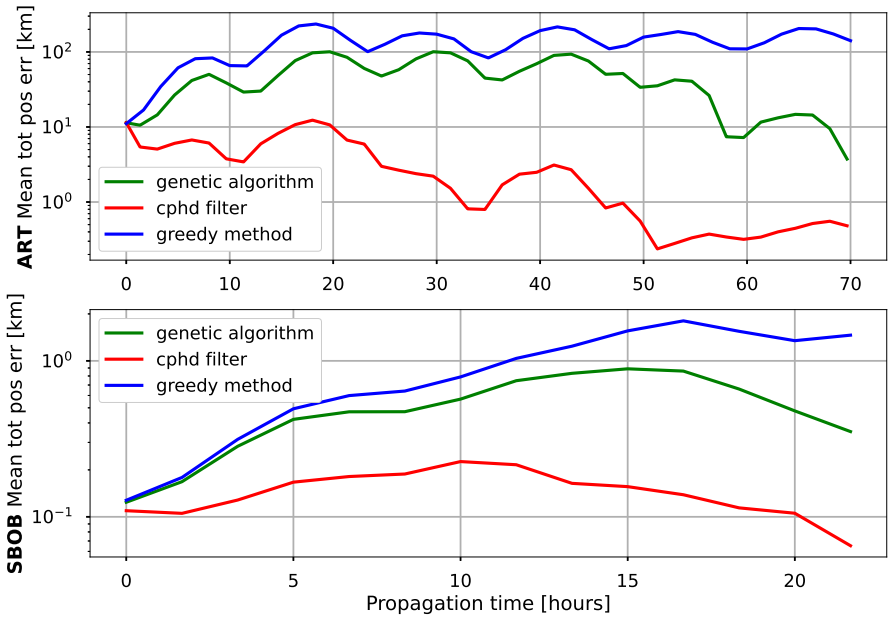

Figure 9. Mean total position error trends for the three methods analysed. In green the genetic algorithm, in red the CPHD filter presented in this paper and in blue the greedy method. The upper figure shows the results for the ART telescope case for three days of propagation, while the figure below shows the results for one day of propagation for the SBOB observer.

different extensions which may make use of the detailed uncertainty information propagated through this method. The method can be extended to trigger additional survey tasks on special or high interest events as close passages (that is a recent integration inside SPOOK as well [18]) or targets of interest [5]. The method can be extended as well for initiation of newly discovered objects to absolve to the Catalogue Generation part of SST.
A comparison of performances has been given also with respect to offline methods for observation scheduling. Differently form the two presented methods, genetic algorithm and greedy method, the CPHD filter scheduling does not require a prior propagation of all the targets through all the scheduling time and allows a better memory consumption.

ACKNOWLEDGMENTS

The author would like to thank all the Master and PhD students who previously worked in the development of SPOOK. He acknowledges and thanks, as well, the valuable help of all the members of the current SPOOK and ART team.

REFERENCES

1. Delande E., Frueh C., Franco J., et al., (2018). Novel multi-object filtering approach for space situational awareness, *Journal of Guidance, Control, and Dynamics* **41**(1), 59–73.

2. ESA, (2017). *SPACE SURVEILLANCE AND TRACKING - SST SEGMENT*. "https://www.esa.int/Our_Activities/Space_Safety/Space_Surveillance_and_Tracking_-_SST_Segment". Accessed: 08/20/2019.

3. Fernandez O. R., Utzmann J, Hugentobler U, et al., (2019). Correlation of Optical Observations to Catalogued Objects using Multiple Hypothesis Filters, (January), 22–24.

4. Fernandez O. R., Utzmann J., Hugentobler U., (2019). SPOOK-A comprehensive Space Surveillance and Tracking analysis tool, *Acta Astronautica* **158**, 178–184.

5. Gehly S., Bennett J., (2016). Incorporating target priorities in the sensor tasking reward function, *Advanced Maui Optical and Space Surveillance Technologies Conference*.

6. Goodrich M. T., Tamassia R., (2015). Algorithm Design and Applications.

7. Grundel D., Murphey R., Pardalos P. M., (2004). *Theory and algorithms for cooperative systems*. Vol. 4. World Scientific.

8. Hill K., Sydney P., Hamada K., et al., (2010). Covariance-based network tasking of optical sensors, in *Paper AAS 10-150 presented at the AAS/AIAA Space Flight Mechanics Conference, February*, 14–17.

9. Hinze A., Fiedler H., Schildknecht T., (2016). Optimal scheduling for geosynchronous space object follow-up observations using a genetic algorithm, in *Advanced Maui Optical and Space Surveillance Technologies Conference (AMOS)*. Maui Economic Development Board Maui, HW.

10. Integral C. B. N., (2017). Bivariate and Multivariate Normal Integrals, *Structural Reliability Analysis and Prediction* **2**, 415–427.

11. Little B. D., Frueh C., (2018). SSA Sensor Tasking: Comparison of Machine Learning with Classical Optimization Methods, *Advanced Maui Optical and Space Surveillance Technologies Conference (AMOS)* `www.amostech.com`, 1–17.

12. Mahler R., (2007). A survey of PHD filter and CPHD filter implementations, *Signal Processing, Sensor Fusion, and Target Recognition XVI* **6567**(1), 65670O.

13. Osweiler V. P., (2006). Covariance estimation and autocorrelation of NORAD two-line element sets.

14. Pardalos P. M., Murphey R., Grundel D., (2004). *Theory and Algorithms for Cooperative Systems*. Vol. 4. World Scientific.

15. Pedone G., (2019). Master Thesis: Strategies and Data Processing for the Optical Observation of Space Debris, *Politecnico di Milano*.

16. Pedone G., Vallverdu Cabrera D., Dimitrova Vesselinova M. G., et al., (2021). Spook: A Tool for Space Objects Catalogue Creation and Maintenance Supporting Space Safety and Sustainability, in */th IAA/UT Space Traffic Management Conference, Austin, Texas*.

17. Ristic B., Vo B. N., Clark D., (2011). A note on the reward function for PHD filters with sensor control, *IEEE Transactions on Aerospace and Electronic Systems* **47**(2), 1521–1529.

18. Schiemenz F., Utzmann J., Kayal H., (2019). Survey of the operational state of the art in conjunction analysis, *CEAS Space Journal* **11**(3), 255–268.

19. Schiemenz F., Utzmann J., Kayal H., (2020). Adaptive Gaussian Mixture based Orbit Determination with combined atmospheric density uncertainty consideration, *Advances in Space Research*, 1–32.

20. Vo B. N., Ma W. K., (2006). The Gaussian mixture probability hypothesis density filter, *IEEE Transactions on Signal Processing* **54**(11), 4091–4104.

21. Vo B. T., Vo B. N., Cantoni A., (2007). Analytic implementations of the cardinalized probability hypothesis density filter, *IEEE Transactions on Signal Processing* **55**(7 II), 3553–3567.